International Journal of Mechanical, Industrial and Aerospace Sciences
ISSN: 2517-9950
Vol:6, No:8, 2012

Heat Flux Reduction Research in Hypersonic Flow with Opposing Jet

Yisheng Rong, Jian Sun, Weiqiang Liu, Renjun Zhan

***Abstract*—**A CFD study on heat flux reduction in hypersonic flow with opposing jet has been conducted. Flowfield parameters, reattachment point position, surface pressure distributions and heat flux distributions are obtained and validated with experiments. The physical mechanism of heat reduction has been analyzed. When the opposing jet blows, the freestream is blocked off, flows to the edges and not interacts with the surface to form aerodynamic heating. At the same time, the jet flows back to form cool recirculation region, which reduces the difference in temperature between the surface and the nearby gas, and then reduces the heat flux. As the pressure ratio increases, the interface between jet and freestream is gradually pushed away from the surface. Larger the total pressure ratio is, lower the heat flux is. To study the effect of the intensity of opposing jet more reasonably, a new parameter RPA has been introduced by combining the flux and the total pressure ratio. The study shows that the same shock wave position and total heat load can be obtained with the same RPA with different fluxes and the total pressures, which means the new parameter could stand for the intensity of opposing jet and could be used to analyze the influence of opposing jet on flow field and aerodynamic heating.

***Keywords*—**opposing jet, aerodynamic heating, total pressure ratio, thermal protection system

I. Introduction

DURING hypersonic fly, hypersonic vehicle will meet serious aerodynamic heating, which burns out the vehicle and defeats the fly mission. It means a lot for hypersonic vehicle to reduce the aerodynamic heating during fly. In last century, Warren [1] suggested using opposing jet to reduce aerodynamic heating for vehicle and did the experiment validity. With the development of the aeronautics and astronautics, the advantage of opposing jet is more and more outstanding. In this century, some scholars kept doing research on this method [2-7]. Hayashi [3-4] did the numerical and experiment study of thermal protection system by opposing jet and obtained some valuable conclusions. The high precise simulation of Navier-Stockes equations was used by Tian [6] to study the detailed influences of the free Mach number, jet Mach number, attack angle on the heat flux reduction and the mechanism was discussed .

Yisheng Rong is with the Engineering Institute of the Armed Police Xi'an 710086, China (e-mail: rong83117@163.com).
Jian Sun is with the National University of Defense Technology, Changsha 410073, China (e-mail: sunjian19850620@163.com).
Weiqiang Liu is with the National University of Defense Technology, Changsha 410073, China (e-mail: liuweiqiang_1103@163.com).
Renjun Zhan is with the Engineering Institute of the Armed Police Xi'an 710086, China.
This investigation was supported by a Major Program of National Natural Science Foundation of China (90916018), a Research Fund for the Doctoral Program of Higher Education of China (200899980006), Natural Science Foundation of Hunan Province, China(09JJ3109), Graduate Innovation Fund of Hunan Province (Grant No. CX2010B004) and the Graduate Innovation Fund of National University of Defense Technology (Grant No. B100102).

In this paper, CFD study on drag reduction in hypersonic flow with opposing jet has been conducted. Flowfield parameters, reattachment point position and surface pressure distributions are obtained and validated with experiments. To study the effect of the intensity of opposing jet more reasonably, a new parameter R_{PA} has been introduced by combining the flux and the total pressure ratio. The study shows that the same shock wave position and aerodynamic drag can be obtained with the same R_{PA} with different fluxes and the total pressures, which means the new ratio parameter could stand for the intensity of opposing jet and could be used to analyze the influence of opposing jet on flow field and aerodynamic heating.

II. Governing Equations and Numerical Methods

A. Governing equations and numerical scheme

In the present study, axisymmetric Navier-Stokes equations are used as governing equations. NND scheme with MUSCL interpolation for convective terms and central difference is used for viscous terms. Full implicit LU-ADI factorization method for time integration is used.

B. Grid and flow conditions

Fig. 1 shows the grid system used in the present study. The number of grid points is 24 in the ξ direction (along the body) and 240 in the η direction (perpendicular to the body). The blunt body is 50mm in diameter, and the nozzle is 4mm in diameter. Table 1 shows the flow conditions.

TABLE I
Flow Conditions

	Free stream	Opposing jet
gas	Air	N_2
Mach number Ma	3.98	1.0
Total pressure P_0/MPa	1.37	0.4~0.8 $P_{0\infty}$
Total temperature T_0/K	397	300
Wall temperature T_w/K	295	

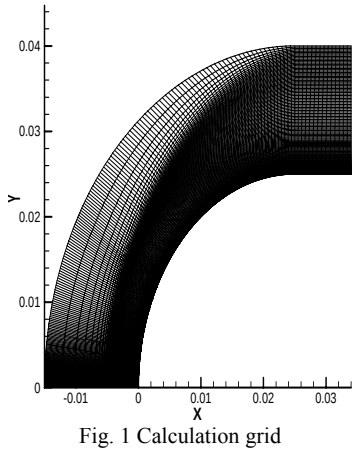

Fig. 1 Calculation grid

III. Numerical Results and Experiment Validation

A. Flowfield

Fig. 2 shows the density distribution in the flowfield which is compared with schlieren photographs.

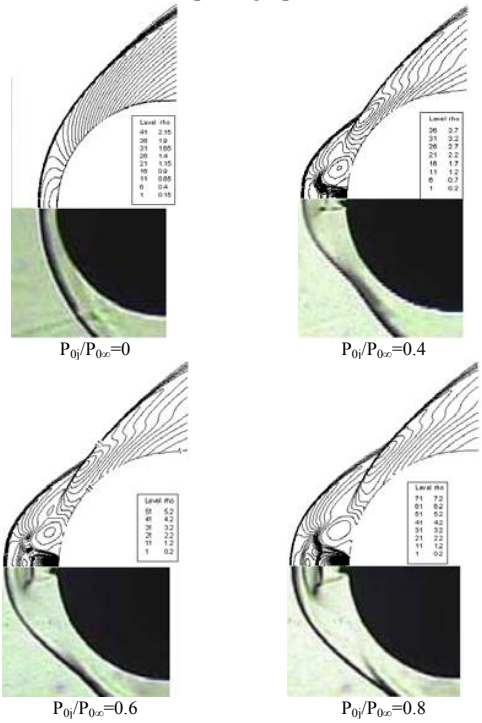

$P_{0j}/P_{0\infty}$=0 $P_{0j}/P_{0\infty}$=0.4 $P_{0j}/P_{0\infty}$=0.6 $P_{0j}/P_{0\infty}$=0.8

Fig. 2 Comparisons between density contours and schlieren photographs

In Fig. 2, the structure of shock waves is complicated. There is a Mach disk in front of the jet outlet. After passing through the Mach disk, the opposing jet interacts with the freestream and forms a thin bow shock. And there is recompression shock wave next to recirculation region. The flowfield characteristics are well simulated numerically. The schlieren photographs validate the correctness of the numerical simulation. And in different total pressure ratio conditions, the positions of Mach disk from simulation results have good agreement with those from experiment results. And the positions of shock wave from simulation results are also the same with those from experiment results. Fig. 3 and Table 2 show other results from numerical simulation. There are other characteristics of the flowfield in Fig. 3 and positions of reattachment points in Table II. With the increase of total pressure ratio, the area of cool recirculation region increase and the position of reattachment point moves away from the stagnation point.

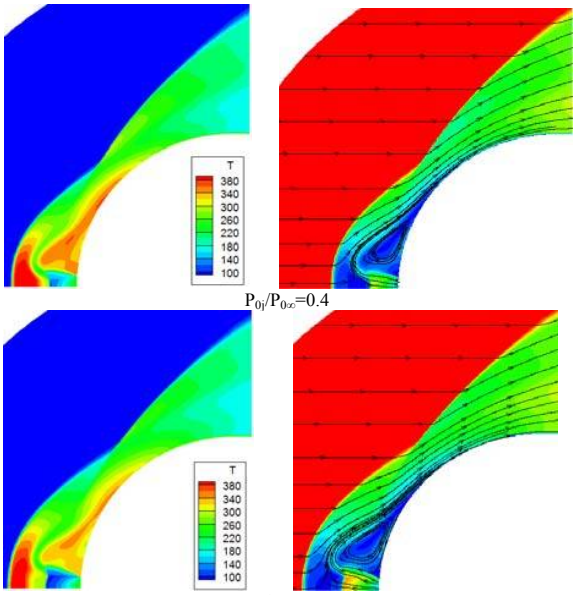

$P_{0j}/P_{0\infty}$=0.4 $P_{0j}/P_{0\infty}$=0.6

Fig. 3 Temperature contours and stream lines

TABLE II
Positions of Reattachment Points

$P_{0j}/P_{0\infty}$	0.4	0.6	0.8
Numerical result	33.7°	35.4°	36.3°

B. Pressure distribution

A surface pressure distribution of the numerical analysis is shown in Fig. 4 and the Positions of peak pressure of different total pressure ratio are shown in Table 3. In the recirculation region, pressure significantly decreases while the opposing jet blows. As the pressure ratio increases, the pressure in the recirculation region gradually decreases. Peak of pressure is located downstream compared with reattachment point.

Fig. 4 Pressure distribution

TABLE III
Positions of Peak Pressure

$P_{0j}/P_{0\infty}$	0.4	0.6	0.8
Numerical result	36.6°	38.2°	38.7°

C. Heat flux distribution

Stanton number St is used to compare each heat flux distributions, which is defined as

$$St = \frac{q_w}{(T_{aw} - T_w)\rho_\infty c_{p\infty} u_\infty} \quad (1)$$

$$T_{aw} = T_\infty \left\{1 + \sqrt[3]{\Pr}\left[(\gamma - 1)/2\right] M_\infty^2\right\} \quad (2)$$

where q_w is surface heat flux, T_{aw} is an adiabatic wall temperature, T_w is the wall temperature, ρ_∞ is the freestream density, u_∞ is the freestream velocity, T_∞ is the freestream temperature, M_∞ is the freestream Mach number, Pr is the Prandtl number, $c_{p\infty}$ is the specific heat at constant pressure and γ is the ratio of specific heats.

A Stanton number distribution of the numerical analysis is shown in Fig. 5, compared with experiment data. And the Positions of peak heat flux of different total pressure ratios are shown in Table IV. In the cool recirculation region, heat flux significantly decreases while the opposing jet blows. As the pressure ratio increases, the heat flux in the recirculation region gradually decreases. Peak of heat flux is located downstream compared with reattachment point.

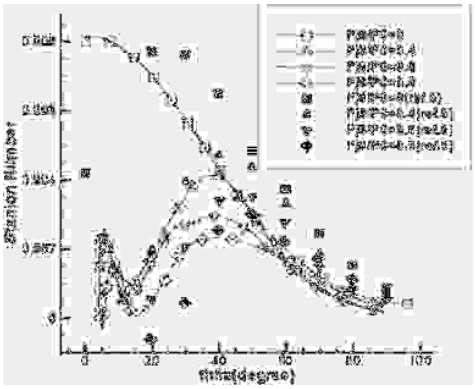

Fig. 5 Distribution of Stanton number

TABLE IV
POSITIONS OF PEAK HEAT FLUX

$P_{0j}/P_{0\infty}$	0.4	0.6	0.8
Numerical result	37.9°	39.2°	39.7°

D. Physical Mechanism of Heat Flux Reduction

When there is no jet, the high speed freestream will interact on the surface directly and the high kinetic energy of the freestream will transform to high temperature to create aerodynamic heating, especially at the stagnation point. When the opposing jet blows, the freestream is blocked off, flows to the edges and not interacts with the surface to form aerodynamic heating. At the same time, the jet flows back to form cool recirculation region, which reduces the difference in temperature between the surface and the nearby gas, which also keeps the surface cool. As the pressure ratio increases, the high energy freestream is gradually pushed away from the surface, and the heat flux in the recirculation region gradually decreases.

IV. Parameter for the Influence of the Opposing Jet on Flowfield

A. New parameter introduced

Total pressure ratio stands for the intensity of the opposing jet. But the intensity of the opposing jet also depends on the flux. It will be more reasonable to combine Total pressure ratio and jet flux. When the jet speed is fixed, the flux depends on the area of the jet outlet. Then a new parameter [7] for the intensity of the opposing jet is introduced, which can be used to analyze the influence of the opposing jet on flowfield.

$$R_{PA} = \frac{P_{0j}}{P_{0\infty}} \frac{A_j}{A_{base}} = \frac{P_{0j}}{P_{0\infty}} \frac{R_j^2}{R^2} \quad (3)$$

Where R_j is the radius of the jet outlet and R is the radius of the blunt body.

Different cases are set to find out how the parameter works. Some of the cases have the same R_{PA} but different flux and total pressure ratio. The setting is shown in Table V.

TABLE V
CASE SETTING OF DIFFERENT R_{PA}

case	R_{PA}	$P_{0j}/P_{0\infty}$	R_j/R	$P_{0\infty}$/ MPa	R/m
A 1.1	0.00256	0.4	0.08	1.37	0.025
A 1.2	0.00256	0.52	0.07	1.37	0.025
A 1.3	0.00256	0.71	0.06	1.37	0.025
A 1.4	0.00256	1.024	0.05	1.37	0.025
A 1.5	0.00256	0.4	0.08	2.055	0.025
A 1.6	0.00256	0.4	0.08	2.74	0.025
A 2.1	0.0032	0.5	0.08	1.37	0.025
A 2.2	0.0032	0.653	0.07	1.37	0.025
A 2.3	0.0032	0.89	0.06	1.37	0.025
A 2.4	0.0032	1.28	0.05	1.37	0.025
A 2.5	0.0032	0.5	0.08	2.055	0.025
A 2.6	0.0032	0.5	0.08	2.74	0.025
A 3.1	0.00384	0.6	0.08	1.37	0.025
A 3.2	0.00384	0.78	0.07	1.37	0.025
A 3.3	0.00384	1.07	0.06	1.37	0.025
A 3.4	0.00384	1.536	0.05	1.37	0.025
A 3.5	0.00384	0.6	0.08	2.055	0.025
A 3.6	0.00384	0.6	0.08	2.74	0.025
A 4.1	0.00448	0.7	0.08	1.37	0.025
A 4.2	0.00448	0.914	0.07	1.37	0.025
A 4.3	0.00448	1.24	0.06	1.37	0.025
A 4.4	0.00448	1.792	0.05	1.37	0.025
A 4.5	0.00448	0.7	0.08	2.055	0.025
A 4.6	0.00448	0.7	0.08	2.74	0.025
A 5.1	0.00512	0.8	0.08	1.37	0.025
A 5.2	0.00512	1.045	0.07	1.37	0.025
A 5.3	0.00512	1.42	0.06	1.37	0.025
A 5.4	0.00512	2.048	0.05	1.37	0.025
A 5.5	0.00512	0.8	0.08	2.055	0.025
A 5.6	0.00512	0.8	0.08	2.74	0.025

B. Influence on the shock wave location

The shock wave location is an important characteristic of the complicated hypersonic flowfield. It is the result of the interaction of freestream and the opposing jet.

Let $x_{Ma=1}/R$ stands for the shock wave location, which is ratio of the distance between the stagnation point and the point where Ma=1 on the symmetry axis to the radius of the blunt body. The results of different cases are shown in Fig. 6, in which A x.1 means A 1.1 to A 5.1 and others means the same way. From Fig. 6, it is known that the shock wave locations for the same R_{PA} are almost the same. Let Err stands for the relative error. And $Err = |x_i - \overline{x}| / \overline{x}$, where $\overline{x} = \sum_{i=1}^{N} x_i \Big/ N$ is the average value. In the cases, the biggest relative error is 2.97%, as shown in Table VI.

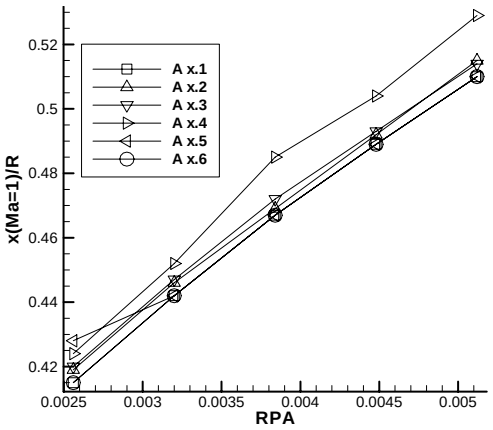

Fig. 6 Shock wave locations of different R_{PA}

Table VI
RELATIVE ERROR FOR SHOCK WAVE LOCATIONS OF DIFFERENT R_{PA}

R_{PA}	average shock wave location	relative error %					
		A x.1	A x.2	A x.3	A x.4	A x.5	A x.6
0.00256	0.420	1.24	0.29	0.05	0.90	1.86	1.24
0.0032	0.445	0.67	0.22	0.45	1.57	0.67	0.67
0.00384	0.471	0.85	0.42	0.21	2.97	0.85	0.85
0.00448	0.493	0.81	0.20	0	2.23	0.81	0.81
0.00512	0.515	0.97	0	0.19	2.72	0.97	0.97

From Fig. 6 and Table 6, it is known that the new parameter could stand for the intensity of opposing jet well on the shock wave location. As R_{PA} increases, the shock wave location $x_{Ma=1}/R$ increases.

C. Influence on the total heat load

In the reduction of aerodynamic heating, it is important to reduce the maximum value of heat flux. Also it is important to reduce the total heat load to the body. The total heat load Q is estimated as an integration of heat-flux distribution over the surface of blunt body as follows:

$$Q = 2\pi R \int_{\theta=20}^{\theta=90} q_w \sin\theta d\theta \quad (3)$$

Where R is radius of nose of blunt body, q_w is surface heat flux and θ is the angle measured from central axis of model.

The total heat load results of different cases are shown in Fig. 7. From Fig. 7, it is known that the total heat loads for the same R_{PA} are almost the same. Let Err stands for the relative error. And $Err = |x_i - \overline{x}| / \overline{x}$, where $\overline{x} = \sum_{i=1}^{N} x_i \Big/ N$ is the average value. In the cases, the biggest relative error is 4.41%, as shown in Table VII.

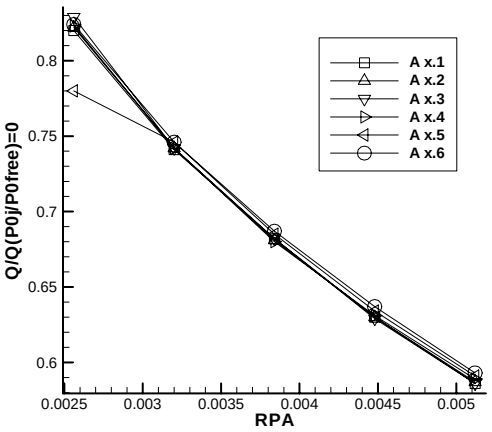

Fig. 7 Total heat load of different R_{PA}

TABLE VII
RELATIVE ERROR FOR TOTAL HEAT LOAD OF DIFFERENT R_{PA}

R_{PA}	average total heat load	relative error %					
		A x.1	A x.2	A x.3	A x.4	A x.5	A x.6
0.00256	0.816	0.49	0.74	1.59	0.86	4.41	0.98
0.0032	0.743	0.27	0.13	0.13	0.13	0.40	0.40
0.00384	0.683	0.15	0.29	0.15	0.44	0.29	0.58
0.00448	0.632	0.32	0.32	0.47	0.16	0.32	0.79
0.00512	0.589	0.51	0.34	0.51	0	0.34	0.68

From Fig. 7 and Table 7, it is known that the new parameter could stand for the intensity of opposing jet well on the total heat load. As R_{PA} increases, the total heat load decreases.

V. CONCLUSIONS

In the present study, heat flux reduction in hypersonic flow with opposing jet is investigated with CFD. The detailed flowfield with opposing jet in hypersonic flow are calculated by solving axisymmetric Navier-Stokes equation. The numerical results are validated with experiments. The remarkable heat flux reduction is observed when the opposing jet flows. To study the effect of the intensity of opposing jet more reasonably, a new parameter R_{PA} has been introduced by combining the flux and the total pressure ratio. The study shows that the same shock wave position and total heat load can be obtained with the same R_{PA} with different fluxes and the total pressures, which means the new parameter could stand for the intensity of opposing jet and could be used to analyze the influence of opposing jet on flow field and aerodynamic heating.

REFERENCES

[1] Warren C H E. "An experimental investigation of the effect of ejecting a coolant gas at the nose of a bluff body", Journal of Fluid Mechanics, 1960, 8: 400-417.

[2] Meyer B, Nelson H F, Riggins D . "Hypersonic drag and heat-transfer reduction using a forward-facing jet", Journal of Aircraft, 2001, 38(4): 680-686.

[3] Hayashi K, Aso S, Tani Y. "Experimental study on thermal protection system by opposing jet in supersonic flow", Journal of Spacecraft and Rockets, 2006, 43(1): 233-235.

[4] Hayashi K, Aso S, Tani Y. "Numerical study of thermal protection system by opposing jet", 43rd AIAA Aerospace Sciences Meeting and Exhibit. Reno, NV, 2005. AIAA 2005-188.

[5] Geng X R, Gui Y W, Wang A L, He L X. "Numerical investigation on drag and heat transfer reduction using 2-D planar and axisymmetrical forward facing jet", ACTA Aerodynamic sinica, 2006, 24(1): 85-89.

[6] Tian T, Yan C. "Numerical simulation on opposing jet in hypersonic flow", Journal of Beijing University of Aeronautics and Astronautics, 2008, 34(1): 9-12.

[7] Rong Y S, Liu W Q. "Analysis of the influence of opposing jet on flow field and aerodynamic heating at the nose of reentry vehicle", ACTA Aeronautica et Astronautica sinica, 2010, 31(8): 1552-1557.